Impact of Sampling on Uncertainty: Semiconductor Dimensional Metrology Applications

Benjamin Bunday[a], Bart Rijpers[b], Bill Banke[c], Chas Archie[d], Ingrid B. Peterson[e]
Vladimir Ukraintsev[f], Thomas Hingst[g], Masafumi Asano[h]

[a]ISMI, CD Metrology, Austin, TX, USA; [b]ASML, R&D, CD Metrology, De Run 6501, 5504 DR Veldhoven, The Netherlands; [c]IBM Microelectronics, Burlington, VT, USA; [d]IBM Microelectronics, East Fishkill, NY, USA; [e]Applied Materials, Silicon Systems Group, Santa Clara, CA, USA; [f]Veeco Instruments, Inc., Santa Barbara, CA, USA; [g]Qimonda, Dresden, Germany; [h]Toshiba Corporation, Process & Manufacturing Engineering Center, Yokohama, Japan

ABSTRACT

The International Technology Roadmap for Semiconductors (ITRS) provides a set of Metrology specifications as targets for each technology node. In the current edition (2007) of the ITRS the conventional precision (reproducibility) is replaced with a new metric - measurement uncertainty for dimensional metrology[1]. This measurement uncertainty contains single tool precision, tool-to-tool matching, sampling uncertainty, and inaccuracy (sample-to-sample bias variation and other effects). Clearly, sampling uncertainty is a major component of measurement uncertainty. This paper elaborates on sampling uncertainty and provides statistical estimates for sampling uncertainty. The authors in this paper address the importance and the methods of proper sampling. The correct sampling captures and allows for the expression of the information needed for adequate patterning process control. Along with typical manufacturing process control cases (excursion control, advanced and statistical process control), several other applications are explored such as optical and electron beam line width measurement calibration, measurement tool evaluations, lithographic scanner assessment and optical proximity correction implementation. The authors show how appropriate choices among measurement techniques, sampling methods, and interpretation of measurement results give meaningful information for process control and demonstrate how an incorrect choice can lead to wrong conclusions.

Keywords: sampling, ITRS, Metrology, OCD, CD-SEM, TEM, STEM, AFM, Uncertainty, matching, accuracy

1 INTRODUCTION

Engineers and scientists around the world use the ITRS[1] as a guideline of metrology and process targets for the successful operation of a semiconductor fabricator at specific technology nodes. Therefore, the ITRS metrology targets are without regard for types of measurement tools, measurement methodology and their foible in making the proper measurement. This is a key problem for the metrologist to solve. Depending on the specific application, a metrologist needs to find proper tool and methodology for measurement of process average (average value for lot, wafer) and process variation (across lot, wafer, field) or dimensions of a specific feature (correlation studies). It is a metrologist's critical duty to define and minimize uncertainty of the measurements to meet the ITRS expectations. Using precision only to assess the performance is not sufficient. Sampling is an important component of measurement methodology which may have a dramatic impact on uncertainty of the measurement. In this paper we present several examples to illustrate the impact of sampling on measurement uncertainty and to give general guidelines of proper sampling for some common applications.

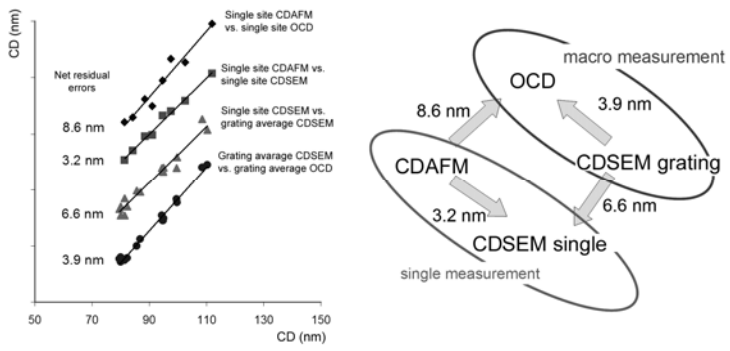

Figure 1: Impact of sampling on Uncertainty for CD-SEM and OCD.

Figure 1 presents the results of linear regression comparisons (tool-to-tool correlations) among the results of various dimensional measurement tools such as critical dimension atomic force and scanning electron microscopes (CD-AFM, CD-SEM) and optical scatterometry (OCD), with measurements sampled and averaged in various ways. With each correlation, the standard error of the residuals (net residual error, NRE) is shown. For display clarity, the y-data for each

comparison has been shifted by a different amount. The top example compares CD-AFM measurements from a single 1 μm by 1 μm size measurement box in each of 8 grating lines of a focus exposure matrix (FEM) compared to optical scatterometry measurements of the same gratings. The light spot size of the OCD is approximately 50 μm in diameter; hence the OCD is sampling over a much larger area than the CD-AFM. In this case the NRE is 8.6 nm. The example second from the top compares CD-AFM and CD-SEM measurements from the 8 gratings where each instrument measured the same location with the same measurement box size. This substantially reduced the NRE to 3.2 nm. The third example compares single site CD-SEM measurements in each grating with the average of 49 measurements by the CD-SEM in each grating. The final example compares the grating average CD-SEM measurements from each grating to the OCD measurements on each grating. The NRE in this case is 3.9 nm. When the variation within the scatterometer grating is not taken into account, the measurement uncertainty estimates are nearly doubled. This example clearly illustrates the impact of sampling methodology on the outcome of tool performance assessment. As more dimensional measurement techniques are being used in semiconductor fabrication, it is now necessary to develop new metrics and methods that provide better ways of metrology tool performance assessment, than that is offered by the conventional, precision-based, simple approach.

2 UNCERTAINTY

The 2007 update of the ITRS Metrology section has changed metrology performance metric from precision to uncertainty. The uncertainty concept has been announced officially by several prominent publications[2] in the early 1990s. The National Institute of Standards and Technology (NIST) helped to spread the use of the uncertainty concept by adopting those documents in a publication of their own.[3] One of the leading concepts embraced by NIST is that of *uncertainty* while moving away from the traditional use of systematic and random errors.

The concept of uncertainty, U, is broken down into two major components called Type A and Type B. That is, there are two major ways to estimate the uncertainty of a measurement. One way is to use traditional statistical methods such as repeatability studies, gauge repeatability and reproducibility (GRR), and analysis of variance (ANOVA). These statistically based methods are categorized as the Type A uncertainty estimates. The Type B uncertainty estimates are everything else not statistically based. An example of Type B uncertainty would be where an engineering estimate can be used to bracket the true value by an engineering-based estimate of the extreme or reasonable bounds. Properly assessing the Type B uncertainty is a critical part of characterizing a reference measurement system.[4] This is due to the need for the reference metrology to have an absolute accuracy assessment. A combined uncertainty estimate can be algebraically expressed as:

$$U^2_{\text{Combined}} = U^2_{\text{Type A}} + U^2_{\text{Type B}} \tag{1}$$

The essential reason for this concept of uncertainty is that the errors can be thought of as having their own uncertainties. Taken from[5], "For example, the result of a measurement after correction (see subsection 5.2) can unknowably be very close to the unknown value of the measurand, and thus have negligible error, even though it may have a large uncertainty." In a sense uncertainty of the measurement is uncertainty of its error. The other key point of the NIST documents is that in some instances systematic errors and random errors maybe estimated using Type A or Type B techniques. *In practice of the majority of instances, the Type B uncertainty assessment is used to estimate the absolute accuracy of a measurement system.* There are some applications, where this estimate is not required.

The NIST Guide[6] also referred to as technical note 1297 (TN1297, specifically Appendix D) does a thorough job of pulling together the international notes on common terms for describing various aspects of uncertainty. A few of the key metrics will be described here. The measurand is the object of the measurement. *Accuracy* is defined as the closeness of the agreement between the measurement result and its [true] value. The TN1297 promotes the use of accuracy as a qualitative quantity, and reserves the use of the uncertainty terminology for associating a quantitative estimate. *Repeatability* is the closeness of the agreement between the results of successive measurement of the same measurand carried out under the same conditions of measurement. Whereas *reproducibility* is the closeness of the agreement between the results of measurements of the same measurand carried out under changed conditions of measurement. *Precision* is defined as "...the closeness of agreement between independent test results obtained under stipulated conditions." Precision encompasses both repeatability and reproducibility.

Note, while the uncertainty of the measurement is better described in terms of Type A and B components, there is often significant value in characterizing the nature of the sample in terms of random and systematic components. In so doing, an optimal sampling plan can be determined. This is further explored in some of the applications in this paper.

In a broad sense, the most fundamental issue of metrology is sampling. Like any real entity, the measurement object has intrinsic properties which can only be partially revealed by a measurement. The metrology instrument examines the object using particular physical principles which by their nature act like a filter to sample a subset of the intrinsic properties of the measurand. So the basic act of measurement is a form of sampling. In selecting the proper instrument technology for a metrology application, attention to the desired measurement property and the nature of the instrument must be paid. However, this is only the first step in appreciating the role of sampling in metrology.

Semiconductor industry applications generally deal with an ensemble of measurement objects. We may wish to know the average value of a line width of a structure across a grating, an exposure field, a wafer, a lot, etc. On the other hand, we may be interested in actually determining good estimates of the variation across these various subgroups of the ensemble. Metrology applications are, indeed, diverse. To accomplish the goals of the measurement exercise, we need to consider a sampling plan of multiple measurements and the analysis to extract the desired information. It is useful to conceptualize the measurement challenge as dealing with four categories of variation: sample variation, single instrument precision, instrument fleet variation (matching), and a fourth category encompassing everything else. While the sources of variation can be parsed in this way, it must be noted that each is affected by the needs of the application and that there are interactions (overlaps) among them (figure 2). The sample variation is the real variation in the ensemble of measurands. The application defines what properties are of interest so in this sense there is an application-sample interaction. The choice of measurement instrument further defines the measurable properties of the sample. At this point it becomes possible to introduce the measurement uncertainty associated with sample variation as filtered by the application and the measurement system. Any particular exercise used to determine this quantity would result in an estimate which we denote by σ_S. To parse measurement variation stemming from the measurement tool into single tool precision and fleet matching terms, it is conceptually necessary to consider the full population of such tools.

The precision is a measure of the measurement variation caused by internal and external noise sources, drifts in electronic components, mechanical motions such as creep and thermal effects. The schematic diagram depicts precision as a circle partially on top of application and sample circles because precision numbers are strongly affected by what needs to be measured as required by the application and the properties of the sample. Any particular exercise used to determine the precision of the measurement instrument would result in an estimate which we denote by σ_P. The tool-to-tool measurement variation is application specific since the application determines that is important to measure. It is also sample specific.

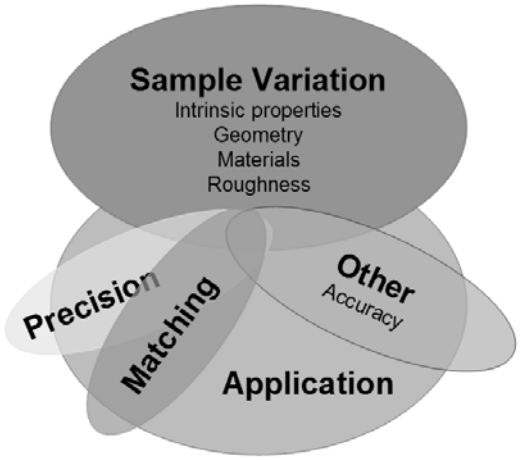

Figure 2: Conceptual representation of uncertainty. The depth order is meant to convey dependencies: most independent is on the bottom. Underlying everything is the application. The application determines what to measure; what is important; and what is not.

For example, if the required measurement is done using a CD-SEM and the sample is very tall, then electron beam tilt variation from tool to tool could lead to systematic measurement differences among tools. Any particular exercise used to determine this quantity would result in an estimate which we denote by σ_m. This quantity could be estimated in a reproducibility exercise where multiple measurement instruments were involved. The analysis would produce the single tool precision estimates by grouping the measurements according to tool and this matching variation estimate by analyzing the full data set without regard to tool and then removing the single tool precision estimate.

Besides the terms so far mentioned there are other sources of measurement variation and inaccuracy which we denote by σ_{other}. This term could include cross correlations among the sources of variation already discussed. Some examples of such uncertainties could be the dependence of tool precision and bias on the set of samples used to estimate them. Another example is a long-term drift of tool-to-tool matching. Other important inaccuracy terms are sample-to-sample bias variation caused by secondary and often uncontrolled process variations and measurement changes as a result of interaction of measurement tool and sample (e.g. resist shrinkage, charging, contamination, buildups). These sample related terms are also dependent on tool selection and are subjects for a long-term drift in tool tuning. Also, we must consider how do engineering and physics constraints of the instrument cause the measurement to fall short of reporting what is actually desired from the measurand. For example, the top/down CD-SEM has weak or negligible sensitivity to

the bottom line width of an undercut structure. Presumably the user will have some idea of the extent of such a situation and can make estimates both for the magnitude of the offset and for the measurement uncertainty associated with it; this uncertainty is an example of Type B uncertainty. This concept is summarized in figure 2 by overlapping circles. Precision, Matching and Accuracy depend on the application and the sample, but also interact with each other.

Given the preceding discussion it is now becomes possible to present an alternative view of the sources of measurement uncertainty as given in Equation (1). Using the notation from Equation (1), the ITRS edition 2007 uses the following formula to estimate uncertainty:

$$U^2_{\text{Combined}} = \sigma^2_S + \sigma^2_P + \sigma^2_M + \sigma^2_{\text{other}} \tag{2}$$

According to Equation (2) combined uncertainty (U_{Combined}) contains the following components: σ_P (precision), σ_M (matching), σ_S (sampling) and σ_{other} (inaccuracy and other effects).

Equation (2) is an attempt to present complex reality in a simplified form. It is understood that the combined uncertainty is a complicated function of time or trial, tool(s) and sample(s) used for the specific measurement. It is important to be aware of the complexity of these relations among different terms of the combined uncertainty. However, from a practical standpoint, splitting the uncertainty into pure independent terms is highly constructive for analysis and for finding ways to improve (reduce) the uncertainty of measurement.

At this point, Equation (2) relates to the combined measurement uncertainty of a *single* measurement by a particular metrology instrument for a particular application. The next step is to discuss a sampling strategy and how sampling can improve the measurement uncertainty of the final result. As an example consider a situation where the precision component dominates the combined uncertainty. This component can be effectively suppressed by measuring a sufficiently large number of members of the population of interest. This is because it is a Type A sources of variation. A byproduct of the Central Limit Theorem[7] says that the variance of the mean for a random variable goes as the variance of the single measurement divided by the sample size, n:

$$\sigma^2_{\bar{P}} = \frac{\sigma^2_P}{n} \tag{3}$$

where $\sigma_{\bar{P}}$ is a one sigma value of the precision uncertainty of the mean.

The uncertainty statement for this example could take the form of an expanded uncertainty of the mean by assigning upper and lower bounds to a confidence interval. The Student t test is typically used to determine these bounds based on a choice for confidence value α.[8] In the following expression $t_{\alpha/2,\,n}$ is the critical value of the Student-t distribution:

$$\left(\text{Lower Bound}, \text{Upper Bound}\right) = \left(\overline{X} - t_{\alpha/2,n}\sigma_{\bar{P}},\ \overline{X} + t_{\alpha/2,n}\sigma_{\bar{P}}\right) \tag{4}$$

This example illustrates a general property of measurement uncertainty: Introducing a sampling plan and working with averages of measurements can reduce many of the uncertainty components. Determining an optimal sampling plan is one of the principal concepts of this paper. To emphasize this we introduce a modified form of Equation (2) by considering all of the sources of variation as variances of averages:

$$U^2_{\text{Combined}} = \sigma^2_{\bar{S}} + \sigma^2_{\bar{P}} + \sigma^2_{\bar{M}} + \sigma^2_{\overline{\text{other}}} \tag{5}$$

We interpret this equation as saying that for a particular application with a particular sampling strategy each of the sources of measurement uncertainty can be suppressed to some degree by averaging. A general statement of the uncertainty bounds for the average measurement can be written as:

$$\left(\text{Lower Bound}, \text{Upper Bound}\right) = \left(\overline{X} - kU_{\text{Combined}}\ \ \overline{X} + kU_{\text{Combined}}\right) \tag{6}$$

where coverage factor k is chosen to meet some confidence level. In the semiconductor industry, k is generally equal to 3 which in the Student-t test translates to a 99.7% confidence level. In the following parts of this paper, we examine various ways of measuring U_{Combined} especially by using sampling and therefore affecting the outcome of these interval estimates. Many metrology applications encountered in the integrated circuit fabrication setting fall into two major categories. In one case the application objective is to estimate the mean of the population and in the other case, the objective is to estimate the variance of the population or more generally speaking, the uncertainty as described by Equation 2. Table 1 shows examples of each with an emphasis on lithographic patterning.

It should be noted that for many applications requiring a mean measurement, there is usually a first step which is to assess the major sources of variation. In the example of a feed-forward application for controlling the formation of the transistor gate, a nested analysis of variance must first be done so the major components of variation are understood[9].This knowledge would dictate how to optimize the sampling plan to result in small uncertainty of the post-

lithography wafer mean which would be used to control a subsequent resist or etch trim process. It is therefore important to be able to estimate the uncertainty associated with a variance determination. Likewise, for the applications shown in the second column of Table 1 the variance, or uncertainty, is the desired estimate. Confidence bounds can be estimated

Table 1: Applications for estimating the mean and variance

Applications for estimating the mean and variance	
Estimation (and associated Uncertainty)	
Mean	**Variance**
❑ Process control (nested ANOVA) ❑ APC (feed forward) ❑ Scanner assessment ❑ OPC ❑ Quality control (lot acceptance) ❑ Calibration	❑ Measurement tool assessment (TMU) ❑ ACLV (process control) ❑ LER (process assessment) ❑ Resist evaluation (LWR) ❑ Fleet matching assessment

using the asymmetric Chi-squared distribution[10]. If the uncertainty expression in Equation 2 is simplified to a single variance term where the variance is estimated from a sample of n measurement, then the following expression for the upper and lower confidence bounds of $U_{Combined}$ are estimated for a confidence value of α, where the $\chi^2_{\alpha/2,\,n-1}$ and $\chi^2_{1-\alpha/2,\,n-1}$ are the critical values for a two-tailed Chi-squared distribution.

$$(\text{Lower Bound}, \text{Upper Bound}) = \left(\sqrt{U^2_{Combined} - \frac{(n-1)U^2_{Combined}}{\chi^2_{\alpha/2,\,n-1}}}, \sqrt{U^2_{Combined} + \frac{(n-1)U^2_{Combined}}{\chi^2_{1-\alpha/2,\,n-1}}} \right) \tag{7}$$

In the practical situation where there are more than two terms in Equation 2 comprising the estimate for the combined uncertainty, the confidence interval estimate is more complicated because of the asymmetric nature of the Chi-squared distribution. A reference is provided to the reader as this calculation is beyond the intended scope of this paper[11]

2.1 Components of sample variation and their impact on uncertainty of measurement

The sample variation is an *intrinsic* property of the product and process. Depending upon how the product is processed, sampling uncertainty may consist of various components of sample (process) variation. The long-term component of process variation is usually determined by lot-to-lot (or batch-to-batch) variation. Short-term process variation or transient component of processing tool tends to be determined through analysis of wafer-to-wafer variation. Other components of process variation are field-to-field (or across wafer uniformity), intra field (patterning uniformity and macro loading effects) and local (microscopic fluctuations) sample variations. It is therefore useful to parse the types of variation into the following components: lot-to-lot (σ_{LT}), wafer-to-wafer (σ_W), field-to-field (σ_F), intra-field (σ_I), and local (σ_L). It is important to note that this parsing is hierarchical, that is, each term captures variation present at one length/time scale and larger but not smaller. The sources of sample variation for these components can come from different physical processes. For example, variation of line width across the photo mask will be common to all exposure fields on all wafers while variation due to the use of different hot plates will be present only from wafer to wafer and lot to lot. The full sample variation (variance) is the sum of all these terms:

$$\sigma^2_S = \sigma^2_{LT} + \sigma^2_W + \sigma^2_F + \sigma^2_I + \sigma^2_L \tag{8}$$

As a simple example to illustrate some of the concepts associated with sampling, consider a situation where intra-field and wafer-to-wafer variations are by far the largest components. Then the expression reduces to

$$\sigma^2_S \cong \sigma^2_W + \sigma^2_I \tag{9}$$

One prudent sampling strategy to minimize the contribution of the sample variation to the estimate of the mean would be to average measurements across several sites per field and several wafers per lot. Let's say N wafers per lot are measured where M measurements per field are gathered. So, from Equation 5, for a single tool, the combined uncertainty of the mean of the N x M measurements would be

$$U^2_{Combined} = \sigma^2_{\bar{S}} + \sigma^2_{\bar{P}} = \frac{\sigma^2_W}{N} + \frac{\sigma^2_I}{NM} + \frac{\sigma^2_p}{NM}, \tag{10}$$

where $\sigma_{\bar{S}}$ and $\sigma_{\bar{P}}$ are the sampling and precision components of uncertainty of the mean, respectively.

How did we come up with these denominators? Because the sample variation terms are hierarchical, suppression of the wafer-to-wafer component does not benefit from multiple measurements per wafer, only from measurements from different wafers. Tool precision, like intra-field sample variation, does benefit from averaging over all measurements. Knowledge of the magnitudes of these sample variance terms and the precision can now be used to choose optimal values for N and M to minimize the combined uncertainty*[1].

In the general treatment consider a sampling of N_{LT} lots, N_W wafers per lot, N_F fields per wafer, N_I lines per field, and N_L measurements per feature. Every component of sampling uncertainty can be reduced through averaging of number of similar samples:

$$\sigma_{\bar{S}}^2 = \frac{\sigma_{LT}^2}{N_{LT}} + \frac{\sigma_W^2}{N_{LT}N_W} + \frac{\sigma_F^2}{N_{LT}N_WN_F} + \frac{\sigma_I^2}{N_{LT}N_WN_FN_I} + \frac{\sigma_L^2}{N_{LT}N_WN_FN_IN_L} \tag{11}$$

Expanding on the notation introduced in Equation (10), we can write this equation in a more compact way as

$$\sigma_{\bar{S}}^2 = \sigma_{\bar{LT}}^2 + \sigma_{\bar{W}}^2 + \sigma_{\bar{F}}^2 + \sigma_{\bar{I}}^2 + \sigma_{\bar{L}}^2 \tag{11'}$$

Table 2 summarizes sampling uncertainty derivatives for several practical cases.

Table 2: Components of sampling uncertainty to be considered per application

Type of measurement	Components of sampling uncertainty	Application
Process average	$\sigma_{\bar{S}}^2 = \sigma_{\bar{LT}}^2 + \sigma_{\bar{W}}^2 + \sigma_{\bar{F}}^2 + \sigma_{\bar{I}}^2 + \sigma_{\bar{L}}^2$	Process characterization
Lot average (N_W, N_F, N_I, N_L>1)	$\sigma_{\bar{S}}^2 = \sigma_{\bar{W}}^2 + \sigma_{\bar{F}}^2 + \sigma_{\bar{I}}^2 + \sigma_{\bar{L}}^2$	Long-term process control
Wafer average (N_F, N_I, N_L>1)	$\sigma_{\bar{S}}^2 = \sigma_{\bar{F}}^2 + \sigma_{\bar{I}}^2 + \sigma_{\bar{L}}^2$	Short-term process control
Field average (N_I, N_L>1)	$\sigma_{\bar{S}}^2 = \sigma_{\bar{I}}^2 + \sigma_{\bar{L}}^2$	Across wafer variation
Site average (N_L>1)	$\sigma_{\bar{S}}^2 = \sigma_{\bar{L}}^2$	Across field variation

So, once the variance components of the process are determined by the nested analysis of variance, a judicious choice of samples can optimally reduce the contribution of the product variation to the measurement.

2.2 Local component of sampling uncertainty

In this section the local (or microscopic) sample variation is further explored. In terms of variability, no sample is truly perfect in the nano-scale realm. In any real process, random variation of feature sizes and profiles occurs due to uncontrollable microscopic variations from many sources. These multiple randomly distributed perturbations, more than can be tracked and controlled, usually converge onto a normal distribution with an average value and a variance, in accordance with the central limit theorem. As introduced in section 2 each metrology technology detects this sample variation uniquely so σ_L is metrology instrument dependent. Consider the examples of the CD-SEM and scatterometer (OCD). The "extent of measurement" of each tool is different—the SEM measures a small segment of line and the scatterometer measures the average CD over a large optical spot, i.e. the tools have different probe sizes. The tools measure different things, or put colloquially, the comparison is one of "apples to oranges". Thus these tools detect variation on different length scales.

This can be made quantitative by considering the true power spectral density (PSD) of line width roughness for the sample of interest. The observed roughness by any particular metrology instrument is given by integrating over the observable region for that instrument. The CD-SEM and OCD observe different regions of this power spectrum. This is illustrated in Figure 3. The OCD is more sensitive on larger periodicities with good estimation of average CD and little sensitivity to small periodicities; while the CD-SEM is more sensitive to smaller periodicities and localized variation.

The situation is a bit more complicated than what has so far been stated. For imaging technologies like CD-SEM, CD-AFM, TEM, and SEM cross section, during a single measurement episode each instrument acts like a band-pass filter in observing the PSD with unique upper and lower cutoff frequencies. The upper cutoff is related to resolution limits of the technology including the probe size while the lower cutoff is tied to the size of the scanned area. For CD-SEM and CD-

*[1] Actually this example is not as simple as it first seems. Consider finding optimum values for N and M such that the total number of measurements, NM, is kept constant. All measurements, regardless of where they are done contribute to the suppression of the intra-field and precision terms. On the other hand, the wafer-to-wafer term can minimized by maximizing the wafers per lot measured. However, measuring multiple wafers comes with an additional throughput hit of load/unload and global alignment actions for each wafer. So the full optimization needs to include a cost constraint.

AFM, multiple probe scans across the measurement region can be either analyzed to estimate the sample roughness within the cutoff frequencies or averaged to suppress the roughness contribution to the measurement uncertainty.

The TEM is a very different imaging technique. The resolution limit is largely determined by the roughness of the sample within the lamella which can have a thickness of around 20 to 50 nm. If only one line cross section is available, the sample roughness cannot be separated from the precision of the instrument. Multiple cross sections improve dramatically the Uncertainty of the measurement[12]. Similar to CD-SEM and CD-AFM, multiple cross sections can be analyzed to provide estimates of sample roughness over the region of the cross sections or averaged to suppress the roughness contribution to the measurement uncertainty.

For non-imaging technologies like OCD, there is clearly a lower cutoff spatial frequency given by the optical spot size, however, the range of roughness detected beyond that is determined by the sophistication of the OCD model. For the common case of a simple unit cell of one line and trench, no roughness can be independently extracted from the single measurement episode. Roughness will affect the repeatability of the measurement and hence be a contributor to the precision of the OCD instrument.

Sampling strategy must also be considered in order to determine what sample variation can be extracted or suppressed. Multiple measurement averaging is an effective way to allow the comparison of results from instruments which sample the PSD in single measurement episodes very differently. For example, with multi-point within-grating averaging, CD-SEM results have often been compared to OCD single measurement results with good correlation. CD-SEM suppliers have introduced multi-point single measurement episode capability to suppress the contribution of roughness on measurement uncertainty. This is further explored in section 4.1.

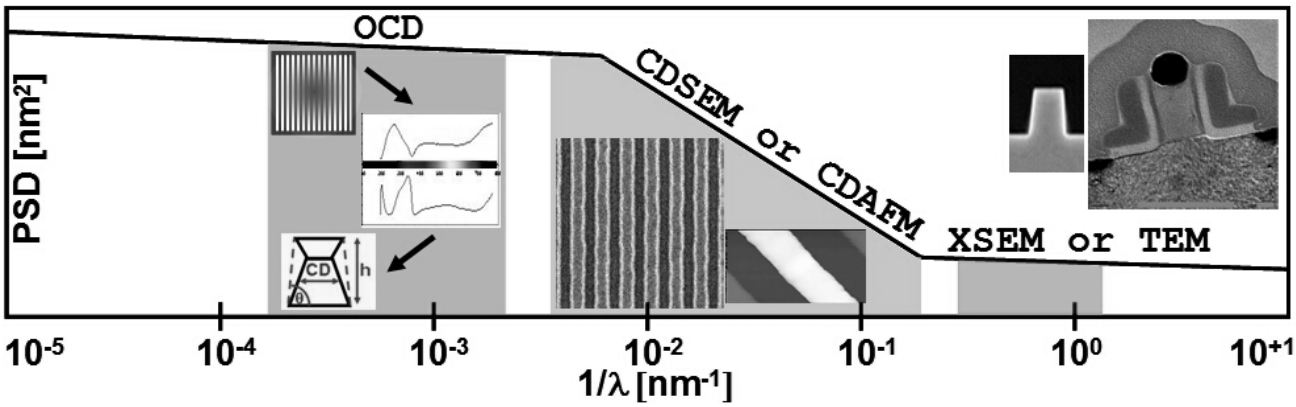

Figure 3: Continuum of CD variation, overlaid by regions of sensitivities of different tool types.

Given these benefits of sample averaging it becomes important to be able to estimate how much averaging is required to achieve a desired measurement uncertainty. Equation (4) was introduced to provide the expression for estimating the error in the mean value of a normal distribution with *n* samples. This can be adapted to produce an expression for determining the number of samples (*n*) to achieve a certain amount of uncertainty ($U_{Combined}$) to a confidence value α on a sample of known variation σ_S with a tool of measurement precision σ_P:

$$n = \left[t_{\alpha/2,n} \frac{\sqrt{\sigma_S^2 + \sigma_P^2}}{U_{Combined}} \right]^2 . \tag{12}$$

Note, the Student-t critical value $t_{\alpha/2,n}$ also depends on *n* but only weakly, so this expression can be iterated to quickly converge on the required value of n. If the desired confidence level is 90%, $t_{\alpha/2,n}$ equals 1.64 for sufficiently large n. In summary the differences among metrology instruments shows most strongly when considering the sample variation on the smallest length scale, σ_L. It is very important to understand the needs of the application, such as the measurement objective (correlation/calibration, SPC, process assessment); how much variation is expected; how important is knowledge of the variation; and how important is the average value. Consideration of these questions determines the choice of metrology instrument as well as the sampling plan. Table 3 lists some applications and considers the importance of local variation and average CD.

Table 3: Different metrology applications and the relative importance of local CD variation and average CD

Application	Local variation important	Average CD important
Real process control for APC	NO	YES
Excursion Control	YES	YES
Scanner qualification	NO	YES
Resist evaluation	YES	YES
OPC characterization	YES	YES
OCD accuracy validation	NO	YES
CD-SEM accuracy validation (using discrete features)	YES	NO

3 MINIMIZING SAMPLE UNCERTAINTY FOR APC AND LOT ACCEPTANCE IN A MANUFACTURING ENVIRONMENT

Automated process control in semiconductors began with the widespread of SPC (Statistical Process Control) in the 1980's followed by systematic Advanced Process Control (APC) implementation from the early 1990's on to minimize yield loss. It consists of applying control strategies and/or employing analysis and computation mechanisms to recommend machine settings for monitoring and regulating a process[13]. APC is now widely adopted for CD control and optimization since the method of using SPC to monitor certain parameters such as gate line width is insufficient[14]. Lot acceptance on the other hand, is commonly used as a go/no go decision applied to production lots during the manufacturing process.

These two applications depend on the ability to minimize the uncertainty in the lot mean CD estimate by using a sample plan that effectively minimizes sampling uncertainty, equation (2) of section 2. Depending on the application, sampling uncertainty may have multiple components; lot-to-lot σ_{LT}, wafer-to-wafer σ_W, field-to-filed σ_F, intra field σ_I and local σ_L, as is described in equation (8) of section 2.1.

3.1 Optimizing the sampling plan; estimating systematic and random components of CD variation

As indicated above, an optimal sampling strategy is critical for both lot acceptance[19] and APC[15,16]. In order to accomplished such strategy, an accurate estimate of the different systematic and random variance components such as lot-to-lot variation, wafer-to-wafer variation within a lot, field-to-field variation within a wafer, site-to-site variation within a field, and pattern-to-pattern within a site for the CD data needs to be achieved. A systematic variation or error is defined as repeating and maintaining the same spatial signature from lot-to-lot whereas a random one changes its spatial signature by lot. As an example, an intrafield CD variation caused by a reticle CD error is systematic since its spatial distribution will remain the same across all lots using this reticle. However, an intrafield variation caused by wafer topography, is considered a random variation since the topography profile changes from wafer to wafer and its impact on the intrafield distribution changes by lot.

As described[19], ANOVA models which assume purely random distributions, do not provide an accurate estimation of these variations when systematic variations are present in the data. A Generalized ANOVA model was developed which addresses this limitation, together with a cost model that evaluates the risks/costs of different sampling strategies to determine the best sampling plan and monitoring schemes for excursion detection.

The concept of optimized sampling was extended to APC[15,16]. In order to quantify systematic (static) and random (dynamic) contributions to the wafer-to-wafer, Intrawafer and Intrafield were extracted by using a general linear model (GLM) ANOVA and the results are shown in Figure 4 for a 90nm CMOS device. The systematic contributions to the CD variation are large, however, these can be compensated by adjustments of tools such as hotplates for intra-wafer and scanner or reticle for intrafield.

As suggested by Asano et al.[18], the amount of random (dynamic) errors impacts the optimal sample size for APC. Assuming the random variances σ_W, σ_F, σ_I as normal distributions, the optimum sample size for N_W, N_F, and N_I to minimize the confidence interval can be estimated given a measurement cost model[17].

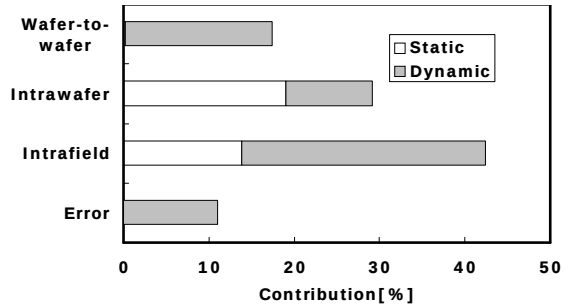

Figure 4: Results obtained by modeling the CD data and extracting the contributions to CD variation.

Case Study

The methodology described above was tested by examining the impact of the sampling plan on the estimation of the lot mean via Monte Carlo simulations[15,16]. Figure 5 shows the comparison of mean+3σ determined by the optimized vs. the conventional sampling plan. An improvement of approx. 60% on the accuracy of the lot mean is achieved.

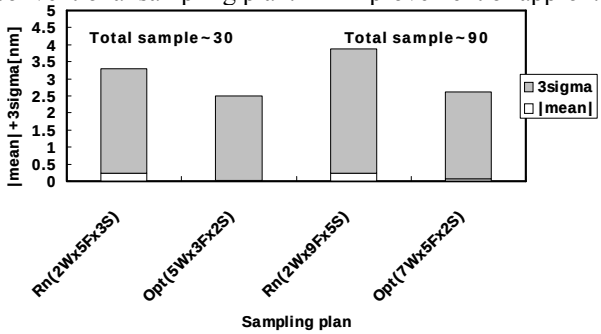

Rn: **conventional sampling plan**

Opt: **optimized sampling plan**

Figure 5: Comparing the impact of the sampling plan on the lot mean

3.2 Optimizing the sampling plan; calculating α and β risks

There is a trade-off in the manufacturing environment when optimizing a sample plan between the material at risk and false alarm risk. The false alarm risk is proportional to the alpha risk, which is the probability of getting an out of control signal from an in-control process. This is also called "producer's risk" or "type I error" in statistical process control literature[18] and below. The material at risk refers to the material exposed to undetected process excursions. The beta risk, "consumer's risk" or "type II error" is the probability of missing an excursion. Similarly, a model that allows a comparison of different sampling schemes on a risk or cost basis is described[19]. Elliott et al looked at the alpha and beta risk family of curves for different SPC control strategies, different sampling plans where the allocation of the number wafers, fields, sites per field varied. In one example doubling the number of fields per wafer reduced significantly the material at risk. In fact at a 3% false alarm rate, normal operating region for the example described, the material at risk was cut almost by half whereas the number of measurements increased by a factor of two.

The alpha and beta risk trade off depends on how large are the individual variances (lot-to-lot, wafer-to-wafer, field-to-field, site-to-site, pattern-to-pattern). We can classify these variances or errors as interchip and intrachip where interchip comprises of lot to lot, wafer-to-wafer, intrawafer and intrafield (supposing several chips in one reticle). The intrachip errors contain local CD error and line edge roughness (LER). The local CD error is defined as a CD shift from a given layout caused by imperfections of optical proximity correction. For example, if the intrawafer or intrafield variances or errors are significantly larger than wafer to wafer, measuring more wafers to detect excursion will not decrease the beta risk whereas measuring more fields will.

The concept of optimizing the alpha and beta risks has been applied to evaluating the risks of trading off scatterometry vs CD-SEM and a detailed description of the theory can be found[18]. Their evaluation for the risks is carried out with operation characteristics (OC) curve, which is the plot of the probability of acceptance $P_a(p)$ versus the percent defective per lot p (the defect level of incoming lot). The curve is generally used for the comparison of sampling characteristics among different sampling plans. Figure 7 shows an example of OC curve. By 100% inspection (all patterns are measured) or the ideal sampling without measurement error, OC curve becomes a step function. In realistic sampling plans, the regions of $1 - P_a(p)$ for $p \leq p_c$ and $P_a(p)$ for $p > p_c$ are considered to relate to producer's risk and consumer's

risk, respectively. By considering the percent defective as a random variable, the ratio of the number of lots suffering type I error per all lots (R_α) and the ratio of the number of lots suffering type II error per all lots (R_β) can be estimated. The R_α and R_β have a trade-off relationship with each other as shown in Figure 6.

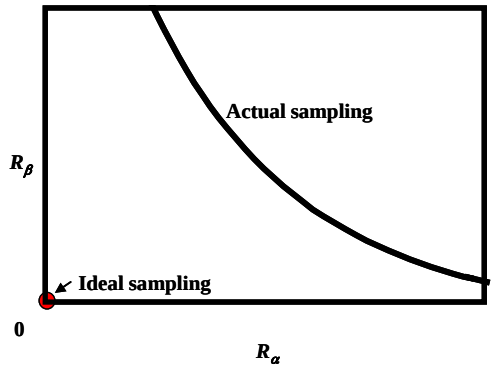

Figure 6: R_α-R_β plot

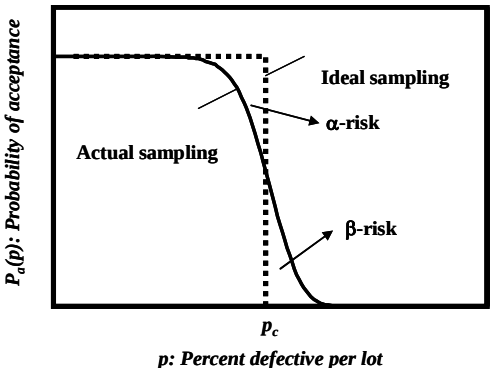

Figure 7: OC curve (p_c is a given criterion whether a lot is accepted or not.)

Case Study

Using Monte Carlo simulation with some assumptions, Asano et al[20]. investigated the risk involved in lot acceptance sampling with SEM metrology and scatterometry.
The assumptions for their case study are:

(a) Scatterometry can measure only grating CD. SEM can measure any type of pattern.
(b) The distributions of interchip CD and of intrachip CD follow normal distributions.
(c) The intrachip CD variation contains all types of local CD errors, including line-end shortening and corner rounding, which a scatterometer is unable to monitor (i.e. the balance of inter- and intrachip CD variation can greatly affect metrology characteristics).
(d) For intrachip and interchip CD variations, three cases are considered (total CD variations are same).
(e) Scatterometry and SEM metrology are well matched (i.e., the average grating CD given by scatterometry and the individual line CD by SEM metrology are always same).
(f) Both metrology tools have no precision errors
(g) Considering the difference of MAM (CD-SEM:scatterometer=2:1), sampling plans per wafer are decided (*i.e.*, MAM x total samples = constant).
(h) A Weibull distribution was used as the probability density function of process capability;
(i) $\bar{x} \pm ks$ is used for the criterion for lot acceptance ($\bar{x}$:,sample mean, s: sample standard deviation, k: a coefficient of positive number). By setting upper and lower specification limits (*USL* and *LSL*), the criterion of lot acceptance is decided.

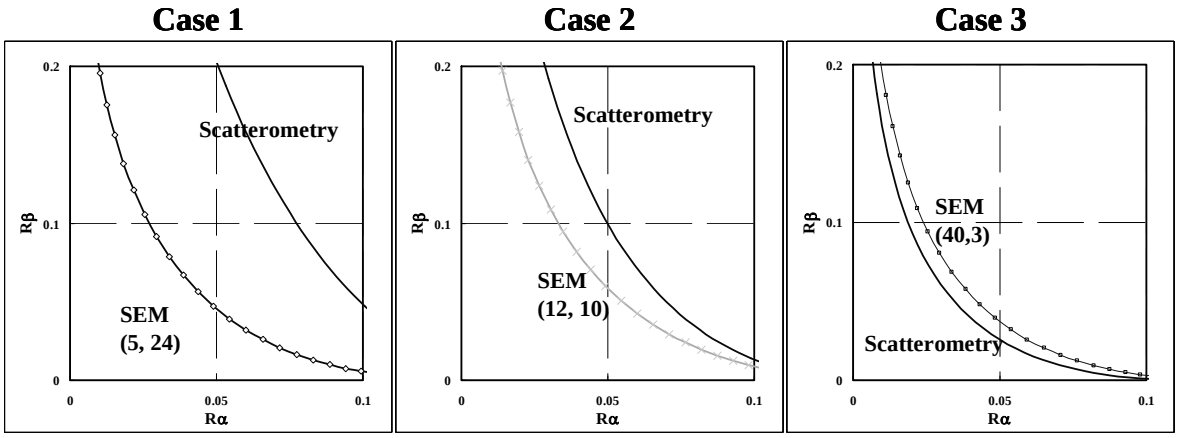

Figure 8: R_α-R_β plots: comparison between scatterometry and CD-SEM (optimized sampling plan). (nc, np) denotes (sampling size for chip, sampling size for pattern)

Figure 8 shows R_α–R_β plot for scatterometry and SEM metrology (with optimized sampling plan). The measurement characteristics depend on the balance between inter- and intrachip CD variation. As intrachip CD variation increases, scatterometry involves a higher risk in spite of the larger sampling size because it is unable to monitor intrachip CD variation sufficiently. In case 3 ($\sigma_c^2 : \sigma_p^2 = 3:1$), scatterometry is better. However, such a case in which interchip CD variation is much larger than intrachip CD variation is considered to be unrealistic because OPC residual errors within a chip, which are emphasized by effective dose and focus error, are a serious problem for CD control in the current manufacturing process. The simulated results suggest that substituting scatterometry for SEM metrology enhances producer's risk and consumer's risk in lot acceptance sampling, such enhancement being particularly marked in the case that intrachip CD variation is larger than interchip CD variation.

4 DIFFERENT APPLICATIONS AND SAMPLING EXAMPLES

4.1 Multiple Feature Measurement for CD-SEM (local sampling uncertainty)

Conventional CD-SEM measurement schemes have utilized measurement of single test features on multiple die on a wafer to log process performance of product at critical stages for processing decisions. These schemes ignore the fact that a single CD measurement is a single sampling of a broader population. Within a given periodic pattern of features which are nominally the same (i.e. a grating) there is a distribution of CD sizes which can be considered "local CD variation". This distribution may or may not be normal (Gaussian) but can be considered so for quantitative treatment. With a larger sampling, the distribution can be characterized to have an average value with a variability, such as line width variation or contact hole variation[21, 22]

Some metrology techniques, such as OCD, are very effective at measuring average CD of a regular grating structure, but do not currently have the ability to characterize the variation within a grating target, beyond possibly flagging a target from a goodness-of-fit metric. Measurement of these variation quantities, which are the result of many measurements of individual features, requires an image-based tool such as CD-SEM. One of the methods coming into use recently with CD-SEMs for improving precision and improving estimation of process mean is averaging over several or many (ideally identical) features within the same image, referenced here as Multiple Feature Measurement (MFM) applications, and sometimes referred to as "Macro CD" or "Average CD". A large amount of data is accumulated from a single scan of a SEM image, providing informative and statistically valid local process characterization. The capability of these applications is improved as the image field of view (FOV) is increased while keeping information density (pixel density) constant. The basic idea behind MFM precision improvement is leveraging the single feature measurement precision by averaging over N multiple features. If x_1, …, x_N are N independent measurements from the same population with standard deviation σ_S, and σ_P is the precision of the SEM measurement of a single feature, the average of these measurements, $\bar{x} = \frac{1}{N}\sum_{i=1}^{N} x_i$, has a standard deviation of $\sigma_{P,MFM} = \sigma_{P,single}/\sqrt{N}$. Thus the MFM measurement precision improves by a $1/\sqrt{N}$ factor. MFM applications also improve the estimation of the process mean and enable estimation of the process variation. Consider a population of features having a Normal distribution of CD, that is, CD ~ $N(\mu,\sigma^2)$. A measurement of a single feature from this population gives little information on the population mean and no information on the population spread. By increasing the number of features we measure (increasing the sample size) we can get a better estimate of the population mean and variation, along with other characteristics of the population. For a group of features with a known population variation σ_S and a tool with single feature precision of σ_P, confidence intervals for the measured value of the mean from N measurements of single features is given by (with 90% confidence).

$$U \cong 1.64 \cdot \sqrt{\sigma_P^2 + \sigma_S^2} / \sqrt{N} \tag{14}$$

To demonstrate the power of this MFM technique, an experiment is reported where a focus exposure matrix (FEM) of contact holes, in photoresist, is analyzed. The targets used had 540nm pitch, so that image FOV ~1.8 μm square were used to image 16 (a 4x4 array) contact holes as shown in Figure 9. The measurement scheme was performed as a typical measurement of across chip CD variation would be run, with 5 measurements per die performed, one in each die corner and one in the center. From the resulting data, Bossung curves, the family of focus curves with varying exposure, are plotted. These can be seen below in Figure 9. The curves are in the order shown in the legend; the heavy lines are the center of the distribution, and the thinner lines are 1σ error bands; 67% of the individual CD distributions lie within these bands. Thus, MFM allows for improved characterization of litho and etch processes. Bossung curves are much "cleaner". Individual hole measurements (see Figure 10, which shows all 16 sets of single hole measurements from the same data

set) would fall anywhere within the error bands shown above; MFM gives a much higher confidence level in the mean of the population of CDs at a given site, and also gives information on the spread of the distribution. The distribution size itself also changes at process window extremities, yielding another metric to monitor process centering. Considering that data such as this is used to choose litho process window, the MFM results are much more appropriate; use of the single CD measurements (as in Figure 10) would be risky.

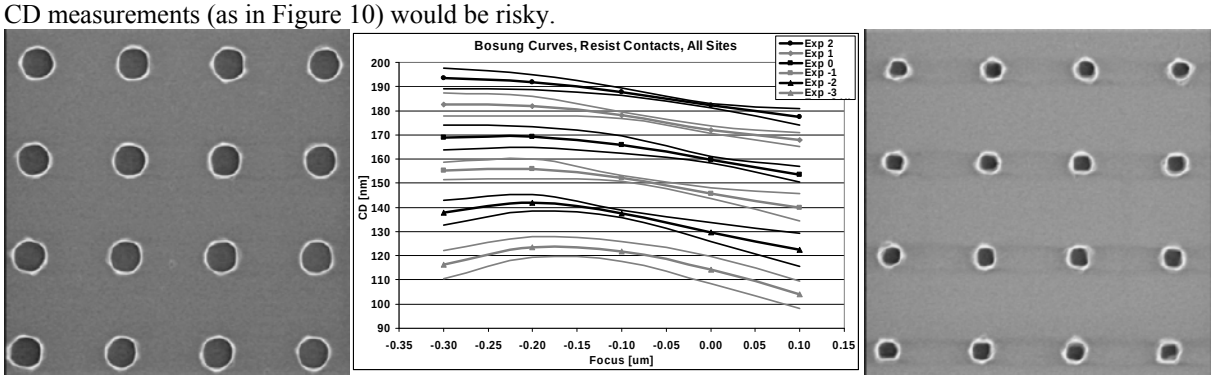

Figure 9: SEM image of resist contact holes at good focus and exposure (left), and resist contact holes at low exposure and poor focus, with increased local CD variation (right). Also, in the middle a Bossung curve using 16-feature MFM for resist contact holes. Each alternating set of black or gray bands is the curve for one exposure value in a FEM, with 1σ error bands.

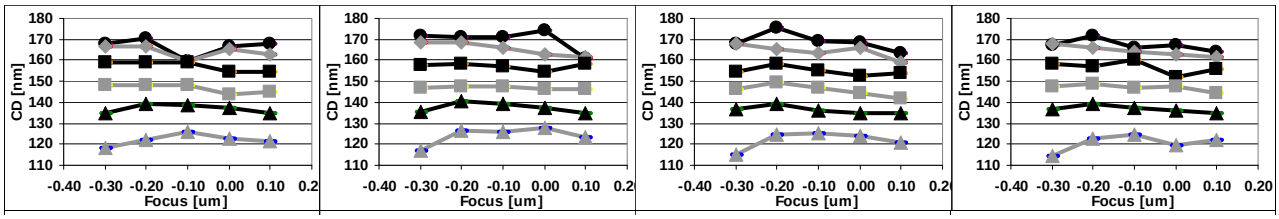

Figure 10: Bossung curves using single CDs, from the 4 of the 16 single etched contact holes within the MFM's in Figure 9. Results include much more noise. Depending on which contact hole is measured, process window selection may greatly vary, and some curves maybe hard to distinguish from others.

4.2 Deep Trench Metrology (local and intrafield sampling uncertainty)

Deep Trench (DT) capacitor based DRAM technology includes several polysilicon fill and recess sequences which define a contact window in the upper part of the DT sidewall to connect the capacitor to the device. As recess etch of polysilicon is known to be sensitive to the etched volume, variation in incoming DT critical dimension (DT CD) will result in recess depth variation. This is a challenge for process control because the recess depth across wafer depends on both the etch process performance (etch fingerprint) and the incoming DT CD (CD fingerprint). This may be addressed by APC, i.e. information on DT CD may be used to adjust the recess etch process conditions (feed forward process control). However, the "averaged" recess depth level is superimposed by local recess depth variation caused by trench-to-trench variations in DT CD. This local depth variation may be (depending on the overall process maturity) a significant contribution to the total within-wafer recess depth variation.

The recess etch process monitoring is currently based on atomic force microscopy (AFM). This instrument allows depth measurement of individual trenches as well as measurement of average depth of an ensemble of trenches (Multiple Feature Measurement, MFM). There are three main application needs (properties of interest) related to this recess depth measurement:

1. *Recess etch process control*: This requires information on tunable parameters to control lot-to-lot variation σ_{LT}, wafer-to-wafer variation σ_W, and potentially field-to-field variation σ_F (within wafer etch fingerprint). At the same time it is essential to separate these tunable parameters from intrafield variation σ_I and local "trench-to-trench" depth variation σ_L which two are random and uncontrollable components.
2. *Process characterization and product quality monitoring*: This requires information on the total range of recess depth across the wafer. This includes information on intrafield variation σ_I and local "trench-to-trench" depth variation σ_L because each individual memory cell has to be within target specifications.
3. *Qualification of the measurement instrument itself*: In order to provide the true metrology tool performance it is required to separate measurement tool precision σ_P from the measurement uncertainty associated with the sample variation σ_S. For AFM this means that the precision test has to be designed in a way that $\sigma_S \approx 0$.

Recess etch process control is a continuous requirement while process characterization and metrology tool qualification may be treated as "one-time activities". Thus, the approach of fulfilling these three application needs may be different. For recess etch process control based on AFM it is required to find an appropriate sampling plan which is compatible with the given metrology tool capacity and throughput. Figure 11 shows the effect of MFM when averaging over a different number of trenches per site at 9 different sites within a field. Measuring a single trench at each site shows the full recess depth range within the field (which is important for process characterization), while averaging over an ensemble of trenches converges to an average recess depth at each site. If the resulting "averaged" intra field variation σ_I is a systematic component showing the same "intrafield fingerprint" in all fields (e.g. based on the DT CD variation as defined by the DT reticle uniformity), measuring one of the 9 sites in MFM mode will fulfill the recess depth process control requirements. On the other hand, a random intra field variation would add a significant component σ_I to the combined uncertainty when measuring only one of the 9 sites. Reduction of this sampling uncertainty component would require intra field averaging, i.e. averaging over an appropriate number of sites within the field to achieve $\sigma_{\bar{I}} \approx 0$. The concept for definition of an optimized sampling plan based on different sources of variation will be discussed later in this paper.

Qualification of the measurement instrument requires a different approach. Repeatability tests show significantly different results depending on the measurement conditions:

1. *Single trench measurement*: This mode shows the worst repeatability performance. Each measurement provides the depth of an individual trench, thus repeated measurements are significantly affected by sampling uncertainty components σ_L and σ_I due to trench-to-trench and intrafield recess depth variations, respectively.
2. *Multiple trench measurements (→ MFM)*: This mode is typically used for process control purposes and averages up to 20 trenches ($\sigma_{\bar{L}} \approx 0$). Repeated measurements are less sensitive to trench-to-trench variations, however intrafield variation σ_I still contributes to the measurement uncertainty because global wafer alignment followed by blind "spot" placement in the DT array does not guarantee measurement of exactly the same trenches in repeated measurements. For tool qualification it doesn't matter if σ_I is a random or systematic component.
3. *High "spot" placement accuracy mode*: This mode uses MFM after a sequence of pattern recognition steps to measure nearly the same trenches. This mode separates measurement tool uncertainty from process variation because $\sigma_{\bar{L}} \approx 0$ and $\sigma_I \approx 0$ and thus provides the true metrology tool performance.

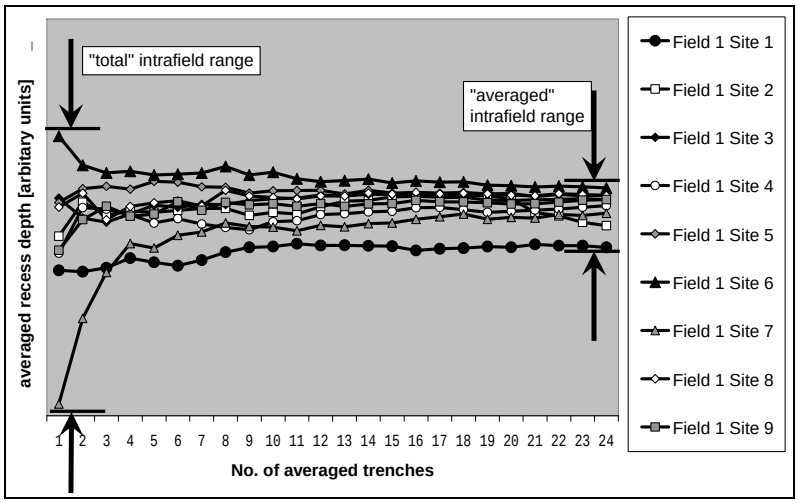

Figure 11: Effect of MFM when averaging over a different number of trenches per site at 9 different sites within a field. Measuring a single trench at each site shows the full recess depth range within the field, while averaging over an ensemble of trenches converges to an average recess depth at each site.

Be aware that $\sigma_I \approx 0$ for tool qualification is not achieved by averaging over several sites within the field (which is required for process control when measuring different wafers) but by the high "spot" placement accuracy mode to measure nearly the same location in repeated measurements on the same wafer. Again, this illustrates the strong dependence of the sampling plan on the application needs.

4.3 Scanner qualification (inter- and intrafield sampling uncertainties)

For scanner qualification we are interested in intrafield CD uniformity caused by the scanner. Other effects such as bake plate non-uniformity need to be subtracted from the data. This can be done when a wafer is measured completely which results in a sampling plan of 5648 points on the wafer. The data is then modeled using an interfield CD model. The results are shown in the most left graph of Figure 12. In this case a hot spot (red zone) and a cold spot (blue zone) are detected, caused by a bake plate non-uniformity. This fingerprint will be subtracted from the CD Metrology data.

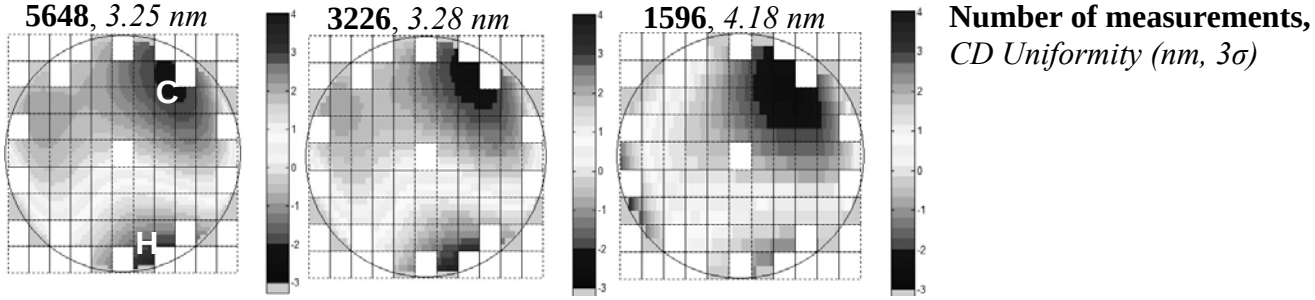

Figure 12: Bake plate CD fingerprint as function of number of measurements. Hot spot (H) and Cold spot (C) are shown.

Smart intrafield sampling schemes will minimize the amount of points to be measured on the wafer while preserving the interfield CD profile on the wafer. This is shown in Figure 12. A full data set (5648 measurements) results in a CD Uniformity of 3.25 nm (3σ) mainly caused by both a hot spot and a cold spot on the bake plate. Reducing the sampling plan to 3226 measurements results in a comparable number for CD uniformity (3.28 nm, 3σ). Further reduction of the sampling plan however results in a different fingerprint: CD Uniformity for 1596 measurements is 4.18 nm (3σ). This is also visible in Figure 12. The first two figures have similar fingerprints, whereas the figure on the right has a different fingerprint. How can we optimize the sampling strategy? This is difficult because local sampling and interfield sampling effects cannot be separated easily. A method to calculate the variation caused by sampling errors and measurement tool precision combined, is described elsewhere[23]:

$$U^2_{\text{Combined}} = \sigma^2_P + \sigma^2_S = 3 \cdot \sqrt{\frac{1}{2N}\sum_{j=1}^{N} \sigma_j{}^2 \{(CD_1 - CD_2)_1, \ldots, (CD_1 - CD_2)_M\}} \qquad (15)$$

First we optimize $U_{combined}$ in formula (15) by minimizing local sampling uncertainty using metrology techniques such as MFM (see section 4.1). Also, Optical CD Metrology can be used. A number of sites on the wafer (N) is measured on a number of wafers in a lot (M). We use two targets which are in the vicinity of each other (CD_1 = Target 1 on a certain location, CD_2 = Target 2 on a location nearby). Effects such as focus/dose errors or reticle errors will be similar for both targets. This offset CD_1-CD_2 is calculated for multiple fields and on multiple wafers. The variation of this offset will give us $U_{Combined}$. With this method we can compare different metrology tools and techniques with each other and find the best one. Now we know the best technique to measure, in this case, a CD fingerprint caused by a bake plate.

Then, we optimize the intrafield sampling plan. We assume that measuring 5648 sites on the wafer will give us a perfect interfield sampling plan (σ_s=0). Therefore, $\sigma^2_{bakeplate} = s^2_{bakeplate} - U^2_{Combined}$. In this formula $\sigma_{bakeplate}$ is the real variation caused by the bake plate, and $s_{bakeplate}$ is an estimator, in this case 3.25 nm (3σ). We calculate $U_{Combined}$ = 1.2 nm from the data by measuring with the full sampling plan (5648) multiple wafers. The real variation of the bake plate is thus $\sigma_{bakeplate}$ = 3.1 nm (3σ) when we use a perfect interfield sampling plan (5648 measurements). Choosing the wrong sampling plan (right hand graph in Figure 12) will result in $s_{bakeplate}$ = 4.18 nm. The interfield sampling error (σ_s) is therefore $(4.18)^2$-$(3.1)^2$ = 2.8 nm (3σ).

4.4 Sampling in Optical Proximity Correction Development

To counter loss of printing fidelity the industry introduces corrections to the basic design intent. Today, a frequent practice is to generate a patterning simulation model that forms the foundation for calculating the corrections needed to ensure printing of all features across a process window needed for a robust manufacturing process. This patterning simulation model must include accurate modeling of the lithography process including the behavior of the resist system as well as the subsequent etch process. To achieve acceptable predictive accuracy, measurements of printed test

structures need to be performed and analyzed to calibrate the model. The CD-SEM is the preferred measurement instrument for this application because of the many different geometries needing measurement. The industry is now developing contour metrology where many CD measurements result from one SEM image of a complex geometry.

Using simple test sites

Examining the fidelity of patterning requires constructing test sites that include a basic geometry of interest along with a neighborhood of other geometries. Examples include: arrays of raised lines/trenches with variable widths and pitches; arrays of end-to-end line/trench ends with variable widths, pitches, and gaps; and arrays of holes/pillars of variable diameter and pitch. There are many others. In order to have examples of all relevant geometries spanning small to large dimensions, a large number of test sites must be designed into test masks or test macros situated in product masks.

Designing an optimal sampling strategy is essential in order to reduce unnecessary measurements and to converge on an acceptable OPC model quickly. Part of this design process includes identifying the critical geometries to measure. The concept of image parameter space is further developed in the next section to explain and quantify critical geometries. We want to avoid under-sampling and over-sampling. In this section other aspects of optimizing the sampling strategy are examined.

The OPC model calibration needs to take into account the variations in patterning coming from factors other than local geometry because data gathered only from one patterning location may not work well for other locations. So across-field, across-wafer, wafer-to-wafer, and lot-to-lot samplings need to be considered. And if other manufacturing process variables are not being sampled by that just mentioned such as different etch chambers, lithography cluster tools, or even different wafer paths within the tools, then the sampling strategy should include these as well. Obviously, there is potential for the sampling plan to grow unacceptable large. The discussion in section 3 on optimizing the sampling plan for production applications is dealing with the same problem but in a different set of applications. Recent work by Han et al[24] attempts to address part of this problem by introducing the concept of an effective sample size. Their idea is that we should consider the sources of variation in determining a sampling plan that maximizes the effective sample size for a given total number of samples. The following example from their paper explains the concept.

Consider an application where the dominant sources of variation can be summarized in the following way:

$$\sigma_S^2 = \sigma_I^2 + \sigma_F^2 + \sigma_W^2 \tag{16}$$

where σ_W is the wafer-to-wafer variation; σ_F, the field-to-field within wafer variation; and σ_I, the intrafield variation. In a three level nested sampling strategy, the total number of samples is given by: $N = n_W \cdot n_F \cdot n_I$, where n_W is the number of wafers, n_F is the number of fields within wafer, and n_I is the number of sites within field. Assuming pure randomness in the choices of wafer, field, and site, the variance of the mean can be written in the following way:

$$\sigma_{\bar{S}}^2 = \frac{\sigma_W^2}{n_W} + \frac{\sigma_F^2}{n_W n_F} + \frac{\sigma_I^2}{n_W n_F n_I}. \tag{17}$$

We now introduce an effective number of samples N_{eff} by requiring the variance of the mean to satisfy: $\sigma_{\bar{S}}^2 \equiv \frac{\sigma_S^2}{N_{eff}}$ (18)

These expressions can be rearranged to produce the following expression for the effective number of samples:

$$N_{eff} = \frac{\sigma_S^2}{\frac{\sigma_I^2}{n_I n_F n_W} + \frac{\sigma_F^2}{n_F n_W} + \frac{\sigma_W^2}{n_W}} \tag{19}$$

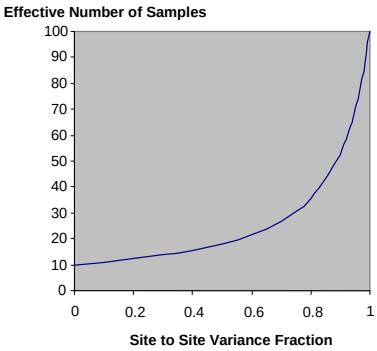

Figure 13: Effective number of samples as a function of site-to-site variance fraction.

The effective number of samples can be calculated once the sampling plan has been determined based on achieving an acceptable measurement uncertainty given a suitable cost model.[9] As an explicit example, consider a sampling strategy in which 10 sites are measured randomly across each wafer and 10 wafers are so measured. For simplicity in this example we are combining intrafield variation with field-to-field variation and calling this site-to-site variation. In Figure 13 we plot the effective number of samples versus the site-to-site to total variance ratio. If the variation within wafer is zero, this variance ratio is zero and the effective sample size is only 10 because all measurements on a given wafer are the same and beyond the first measurement contain no additional information. At the other extreme, if the wafer-to-wafer variation is zero, then all 100 measurements are useful for characterizing the site-to-site variation or for reducing the uncertainty estimate of the mean.

Using contouring

As an alternative to the growing number of measurements needed when using the simple test sites methodology, capturing a relatively few number of contours from SEM images of complex test sites or even in functional designs promises to improve model calibration results and reduce CD-SEM usage. This section briefly explains the fundamental concepts of OPC contouring.

The goal for all model calibration processes is to capture the design intent in the calibration test pattern. For example, a test pattern intended to calibrate an OPC model for an SRAM, flash, or DRAM design would incorporate an array of bit cells of that exact design thereby guaranteeing the design intent is captured in the model. The essential image properties of these unit cells of the design intent can be characterized by a few image parameters. Figure 14 and Figure 15 explain the image-parameter concept. The image parameters are quantified from aerial intensities as minimal intensity (I_{min}), maximum intensity (I_{max}), *slope,* and *curvature factor* of the intensity variation at the CD threshold. Each unique feature produces a unique set of image parameters that quantifies its distinctiveness.

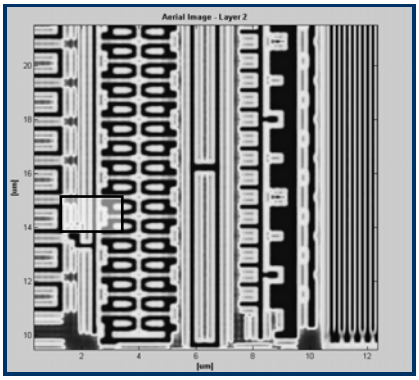

Figure 14: Aerial-image of each location is influenced by the proximity effect. If we cross section this image (See rectangle) we can extract local parameters of the simulation (I_{min} , I_{max}, Slope)

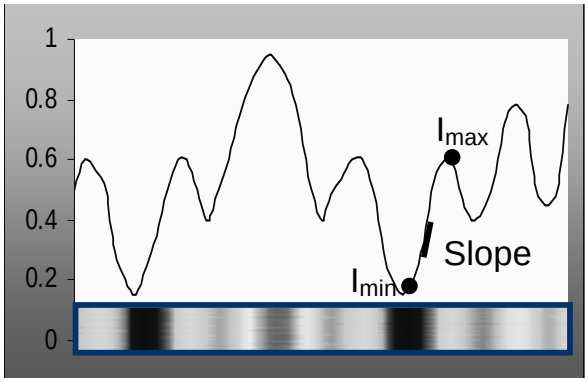

Figure 15: Aerial-image parameters (Imin, Imax, slope) are influenced by the proximity effect.

The following example has been extracted from Vasek et al.[25] Once the image parameters are quantified, the goal is to map the image-parameter space (IPS) for the calibration database and the design database. Figure 16 is a representation of IPS coverage for a calibration test pattern and design database for I_{min}/I_{max} on the left and slope/I_{max} on the right. Note that image parameter space has four dimensions and this figure is showing only two 2-dimensional projections of that space. The pyramids are points from the calibration database and the diamonds are IPS points from the design database. Although the models have interpolation and extrapolation capability, an ideal model would have calibration IPS coverage with the granularity and range that exceeds the design database. The darkened regions in the figure identify areas where the calibration database is not providing good IPS coverage. By using realistic designs in contour based calibration the IPS coverage can be substantially improved while reducing the CD-SEM tool usage. This should lead to

an improved OPC model. More details about the advantages and challenges of contour based metrology can be found in the reference.

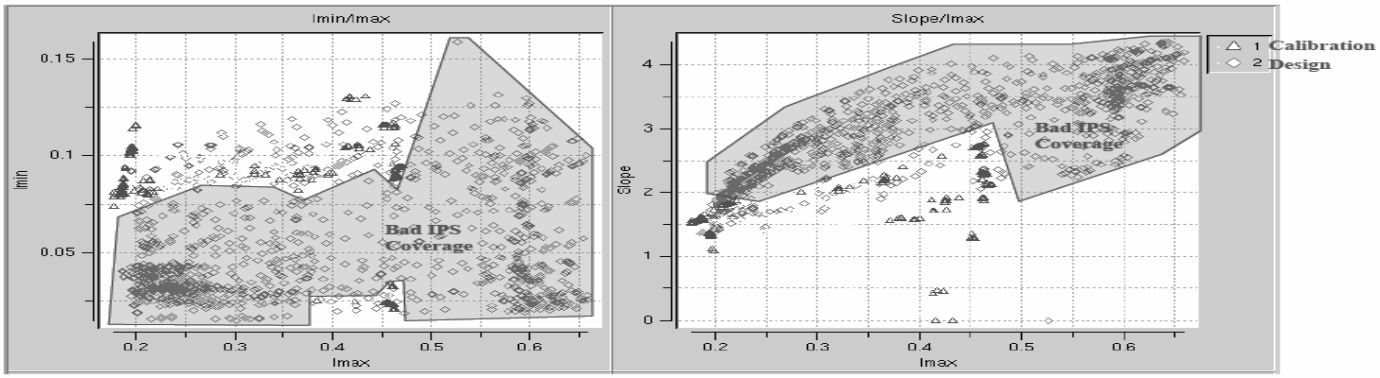

Figure 16: Image parameter space (IPS) plots for image parameters I_{min}/I_{max} (Left) and slope/I_{max} (Right). The pyramids are IPS points from the calibration test pattern and the diamonds are from the design database. The ideal model would be calibrated with a test pattern that contains IPS coverage with the granularity and range of the calibration.

4.5 Scatterometry accuracy validation

For years, scatterometry (OCD) has demonstrated its capability to determine CD and cross sectional profile over periodically aligned line and space (i.e. grating) structures with superior precision. However, to gauge the true capability of scatterometry for process monitoring and to prove that the OCD measurement tracks a process's real physical changes, it is important to gauge the accuracy of the measurement application. Accuracy is defined as the correlation between a tool under test (TuT) to a reference measurement system (RMS) on a set of samples which is representative of the process to be measured. One good metric for accuracy is Total Measurement Uncertainty (TMU)[26], which gives a mean value of the residuals of a tool correlation study between the TuT and RMS. The methodology of implementation of TMU has been discussed in separate articles[27,28,29]. Note that TMU is actually nothing other than $U_{Combined}$ as defined in equation 2 of section 2, with $\sigma_M = 0$ since matching is a non-issue in this case. It thus includes components of σ_P, σ_S and σ_{other}, with σ_{other} representing the non-linearities of the accuracy correlation.

The TMU methodology contains one more important concept especially relevant to the emphasis of this paper on sampling, namely, process stressed artifacts (PSA). In order to properly assess a metrology instrument the set of measurement structures should include examples of all kinds of variations expected to be encountered, sample-to-sample and over time. By intentionally varying relevant process control knobs in their construction, PSA's provide a realistic test of metrology instruments. For the same reason, PSA's are the recommended samples to use in tool matching exercises to give an unbiased estimate of σ_M.

A well executed example of such a calibration exercise is already published [30,31] where ISMI uses their Unified Specification[28] to evaluate OCD tools. In these evaluations, different models for line width and profile are tried, and the model which exhibits optimal TMU is the one which is ultimately used for rating tool precision and accuracy. This iterative technique is powerful, as it helps decide which model is correct by including accuracy in the decision process. When implementing a quality metrology regimen, this exercise is also what should be done when selecting the best model for scatterometry implementation in a production environment for a given production process.

There are great advantages to having a quality set of reference measurements for OCD accuracy validations. TMU can be used in optimizing model building, and metrics for accuracy can be calculated. There are two major considerations for quality reference measurements for correlating to OCD tools. The first is that the OCD tools measure a grating by illuminating it with a beam of light of a moderate diameter such that many features within the grating are sampled in a single measurement, yielding an average measurement. Thus, reference measurements by image-based tools such as CD-SEM or CD-AFM must include many samples over the grating to properly capture the average CD. The second consideration is that due to the good precision performance of OCD tools, the reference measurements of the grating must have a very good (i.e. comparable or better) precision performance. Only then accuracy and TMU metrics will have a meaning. This can be achieved by a large number of measurements, as precision of the mean value estimation will go as $1/\sqrt{N}$ of single feature measurement precision.

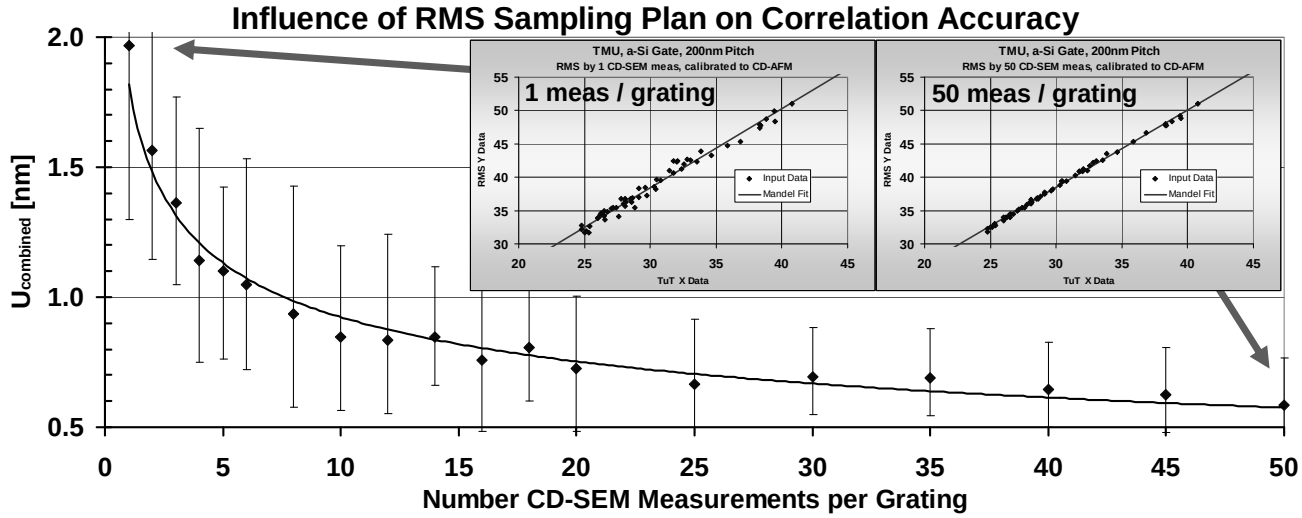

Figure 17: Influence of RMS Sampling Plan on Correlation Accuracy. Inset plots include correlations of OCD to CD-SEM/AFM combination in a-Si gate experiment, with reference measurements represented by 50 CD-SEM measurements (right) and 1 CD-SEM measurement (left). This is an excellent example illustrating how sampling error component σ_S influences $U_{Combined}$, as σ_S is directly dependent on the number of CD-SEM measurements per grating on the x-axis.

In the quoted work[31], such a correlation was performed. The target was etched amorphous Si (a-Si) lines of 200nm pitch with CDs from 25-50nm. Various models were tried, with the best model selected based on TMU minimization. The RMS in this case was a two-step correlation, a combination "CD-SEM / CD-AFM team", where CD-SEM was correlated to CD-AFM for absolute accuracy, and then the gratings were measured thoroughly with the now-calibrated CD-SEM, with 50 measurements per scatterometry grating. These statistics achieve a very high precision of measurement of the average CD of the grating, which is, in effect, the "measurement resolution"; final values are ~0.15 nm for the etched wafers. In the insets in Figure 17, sample correlations can be seen.

To demonstrate the importance of proper sampling in achieving such accurate correlations, further analysis of this same data set has been performed, where different subsets of the CD-SEM measurements were substituted as the reference measurements into the correlation to see how negatively various lesser sampling plans impacts the achievable TMU. It can be seen that the TMU was significantly impacted when N, the number of CD-SEM samples per grating, was less than 15 or 20. Thus it is important that the sampling be chosen properly, or else the results will be poor. It should be noted that the samples used here had a LWR of ~5nm, which is somewhat large by today's standards but not hugely so. A smoother sample might allow for a smaller N to achieve good TMU.

4.6 Overlay APC

A sampling plan for regular (10 parameter) overlay process corrections will in general not be sufficient to capture higher order process offsets (See Figure 18) that can be induced by e.g. etch or rapid-thermal annealing processes.

To show the effect that the sample scheme has on how well the measurements can be used to correct let us look at overlay residuals after correcting with the same higher order overlay model based on measurement data from different sample schemes. The sample schemes are shown in Figure 19. The leftmost sample scheme is chosen by 'just' increasing the number of measurements, especially at the edge of the wafer where the effects are most pronounced. The other two sample schemes are sub-sets of this sample scheme, they are constructed by reducing the number of measurements while maintaining the overall coverage of the wafer.

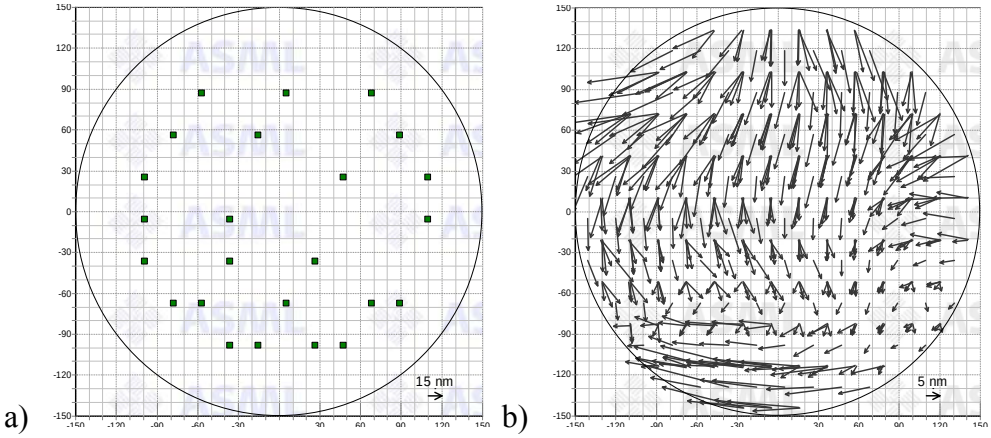

Figure 18 a) Overlay metrology sampling plan for regular process corrections. b) Example of on product overlay measurements showing a higher order fingerprint across the wafer.

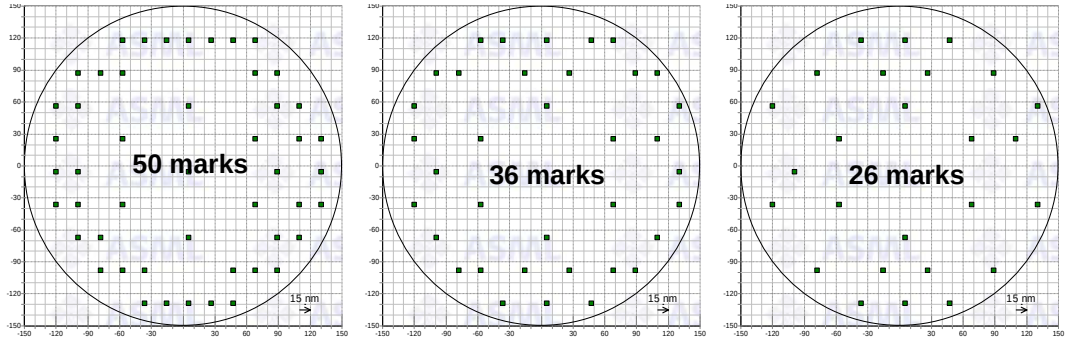

Figure 19: Different Mark layouts (50, 36 and 26 mark sampling plans)

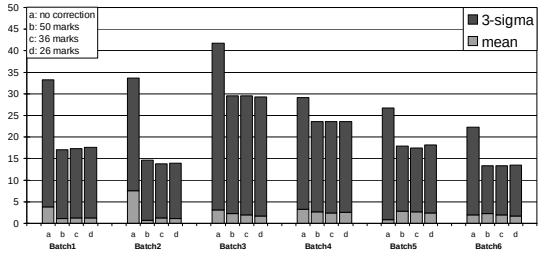

Figure 20 shows overlay residual results (3σ) on 6 typical batches with no corrections applied (case a) and using higher order corrections based on the described sample schemes (case b to d). Sampling more marks (50) will indeed result in a decrease in residuals. It should be noted however that using a subset of this sampling plan the overlay residuals will not get worse. In fact, with the same number of measurements as used for regular corrections the higher order process corrections can be determined with sufficient accuracy.

Figure 20: Overlay residuals (nm) of three different sampling plans.

This illustrates that it's not just the number of measurements that influences the accuracy of metrology APC corrections, but also the distribution of the measurements.

5 CONCLUSION

The 2007 ITRS Metrology chapter includes a new framework for uncertainty, where "uncertainty" replaces the "precision" used in pre-2007 versions. One purpose of this paper has been to communicate and explain this new definition to the worldwide metrology community, as the authors were all complicit in this change. This new definition has been a main topic in the ITRS Metrology Technical Working Group (TWG, of which the authors are all active participants) and ISMI Advanced Litho Metrology Group (AMAG) meetings over the last couple of years. Much spirited discussion has gradually ended in consensus, including both IC manufacturers and equipment suppliers. This new framework eliminates past confusion about matching and accuracy as they pertained, through vague footnotes in the text, to the old precision definition. It makes the key metrics compatible with SEMI standard definitions. Likewise, it shows that sampling is also a major error component in many measurements. The ITRS is supposed to be applicable to any research, development or manufacturing measurement, and thus must include very flexible metrics which can be applied

to any case. The new uncertainty definition (equation 2) includes precision, matching, accuracy and sampling components; it is left to the user to determine which components are important to a given case for defining uncertainty.

It should be noted that in a SEMI E89-defined tool gauge study[32], uncertainty due to "product variability" (i.e. due to real changes in the measurand, which is the sample component of the uncertainty) are not to be included, or at least to be minimized, when rating a tool's general gauge "measurement system variability", i.e. sample uncertainty is not to be attributed to the metrology tool in these cases. Referring to equation 2, this is the case for the precision (σ_P), matching (σ_M) and accuracy (σ_{other}) components used here; however, the new uncertainty definition ($U_{combined}$) includes the sample variation (σ_S) and thus, when σ_S is present, this can be considered a measure of what SEMI E89 terms "total variability". Note that σ_S is the subtle difference in judging a tool to be appropriate for measuring a set of gauge standards or for a set of particular applications, as the sampling error generated by a particular tool/product combination can be very significant and thus make certain metrology tool choices better than others, especially when much small-scale sample variation (i.e. roughness) exists. Thus sample variation is included in the ITRS uncertainty definition specifically to address such cases. When judging compliance with general ITRS roadmap values, it is left up to the user to decide when use of σ_S is appropriate, but the new definition makes this framework available to the user. When doing generic tool testing for ITRS node compliance, it is advisable to separate the tool variability from the product variability. See the "Measurement Equipment Assessment" item in Table 4; a finite set of gauge study artifacts and measurement locations (a closed set) will, by default, ensure that $\sigma_S \approx 0$. When doing specific application testing for a user's manufacturing application with an infinite selection of possible measurement sites, total variability may be the better choice.

After explaining the new ITRS uncertainty scheme, this paper elaborates on sampling uncertainty, addresses the importance and the methods of proper sampling, and provides statistical estimates for sampling uncertainty. Correct sampling captures and allows for the expression of the information needed for adequate patterning process control. Along with typical manufacturing process control cases (excursion control, APC or SPC), several other applications are explored, through examples, such as optical line width measurement calibration, measurement tool evaluations, lithographic scanner assessment and optical proximity correction implementation. In all cases, appropriate choices among measurement techniques, sampling methods, and interpretation of measurement results give meaningful information for process control; likewise, an incorrect choice can lead to wrong conclusions.

The various components of sample variation have different importance in different applications (process targeting, long-term SPC, short-term process variation or wafer-to-wafer monitoring, across wafer variation, across field variation, single site measurement). Also, depending on the application, the sampling uncertainty may be related to a single measurement or to a measurement of the mean of several measurements. In a new, sophisticated way of thinking about process variation, we may consider variation as a general manifestation of the roughness phenomenon, carried out as a continuum through all wavelengths, large and small. This roughness continuum can be described by a Fourier power spectrum. Different metrology tools are sensitive to different parts of this power spectrum (i.e. frequency bands), thus explaining how different metrology tools see different amounts and scales of process variation and detect the process mean to varying uncertainty levels. For process control in a manufacturing environment (APC, lot acceptance) an optimal sampling strategy is critical, thus an accurate estimate of the different systematic and random variance components for the parameter of interest needs to be achieved. The sampling plan can be optimized by considering the variance components. There is a trade-off between the material at risk and false alarm risk, thus a risk evaluation is needed to determine the sampling plan for lot acceptance.

Multiple Feature Measurement (MFM) applications are a prime illustration of how the sample variation σ_S can be defined and quantified. The OCD calibration example takes this a step further and demonstrates how σ_S influences $U_{combined}$; it also shows that the commonly-used TMU metric fits well into the framework of the definition of $U_{combined}$. Depending on the application and on the sensitivity of the measurement tool to different parts of Fourier power spectrum, different approaches may be required for separation of tool variability from product variability. Using a metrology tool which is sensitive to local variation, the impact of the product variability (e.g. σ_I intrafield variation) on process control may be reduced by averaging over several measurements or measurands, while for measurement equipment assessment the same uncertainty component σ_I may be reduced by measuring exactly the same feature in repeated measurements. In other applications, not only the number of measurements is important, but also the distribution of the measurements is an important aspect of the sampling plan. To conclude, the following table summarizes the uncertainty and sampling issues for many of the examples given in this paper and a couple of new examples not covered, such as fleet matching and LER assessment. Table 4 attempts to lay out a simplified form of the complex problem of properly sampling for a very different set of applications found in the semiconductor industry. The

table shows three fundamental considerations associated with each application. The goal of the application is the type of estimation. The diversity of combined uncertainties are shown in the third column, and the last column shows how the combined uncertainty is incorporated to determine a confidence interval for the type of desired estimate.

Table 4: Combined Uncertainty Expressions and Expanded Uncertainties for Various Applications

Application	Estimate Type	Combined Uncertainty Expression	Confidence Interval (Lower bound, Upper bound)
Process control of gate LW	Mean	$U^2_{Combined} \cong \frac{\sigma_W^2}{N} + \frac{\sigma_I^2}{NM} + \frac{\sigma_p^2}{NM}$ or equivalently $U^2_{Combined} \cong \sigma^2_{\bar{W}} + \sigma^2_{\bar{I}} + \sigma^2_{\bar{p}}$	$\left(\bar{\bar{X}} - kU_{Combined}, \bar{\bar{X}} + kU_{Combined}\right)$
Measurement equipment assessment (e.g. TMU)	Variance	$U^2_{Combined} = \sigma_P^2 + \sigma_{other}^2 + \sigma_S^2$ where by design, $\sigma_S^2 \approx 0$	$\left(\sqrt{\frac{(n-1)U^2_{Combined}}{\chi^2_{(n-1),\alpha/2}}}, \sqrt{\frac{(n-1)U^2_{Combined}}{\chi^2_{(n-1),1-\alpha/2}}}\right)$
Fleet matching assessment	Variance	$U^2_{Combined} = \sigma_P^2 + \sigma_M^2 + \sigma_S^2$ where by design, $\sigma_S^2 \approx 0$	same as variance example
LER	Variance	$U^2_{Combined} = \sigma_P^2 + \sigma_S^2$	same as variance example
Scanner assessment	Mean	$U^2_{Combined} = \sigma^2_{\bar{P}} + \sigma^2_{\bar{S}}$	same as mean example

6 REFERENCES

ISMI Technology Transfer documents mentioned are non-confidential and can be viewed at www.sematech.org.

[1] International Roadmap For Semiconductors (ITRS), http://www.itrs.net/Links/2007ITRS/2007_Chapters/2007_Metrology.pdf

[2] *Guide to the Expression of Uncertainty in Measurement*, International Organization for Standardization, Geneva (1995) and "U.S. Guide to the Expression of Uncertainty in Measurement", *American National Standard for Calibration*, ANSI/NCSL Z540-2-1997

[3] B. Taylor, C. Kuyatt, Guidelines for Evaluating and Expressing the Uncertainty of NIST Measurement Results, *NIST Technical Note 1297*, 1994 Edition

[4] L. Lauchlan, et al, Metrology Methods in Photolithography, *Handbook of Microlithography, Micromachining, and Microfabrication, Vol. 1: Microlithography*, P. Rai-Choudhury, Vol. 1, pp. 475-595, SPIE Optical Engineering Press, Bellingham, WA, 1997

[5] ibid from reference 3

[6] idid from reference 3

[7] Central limit theorem: Abraham de Moivre, *Miscellanea Analytica*, , p 26-42 , London, 1730

[8] J. Mandel, *The Statistical Analysis of Experimental Data,* Interscience, New York, 1964

[9] W. G. Cochran, Sampling Techniques, 3rd Edition, John Wiley & Sons, Inc., 1977

[10] G. Snedecor, W. Cochran, *Statistical Methods*, 6th Edition, The Iowa State University Press, Ames, Iowa, 1967

[11] F. Graybill, C. Wang, Confidence intervals on Non-negative Linear Combinations of Variances, *Journal of the American Statistical Association,* Vol. 75, No. 372, December 1980, pp. 869-873

[12] B. Rijpers, E. Langer, D. Verkleij, Automated TEM sample preparation on wafer level for Metrology and Process Control, Proceedings of the International Symposium for Testing and Failure Analysis, November, 2007

[13] J. Moyne, H. Hajj, K. Beatty, R. Lewandowski, SEMI E133: The Process Control System Standard: Deriving a Software Interoperability Standard for Advanced Process Control in Semiconductor Manufacturing, IEEE Trans. On Semiconductor Manufacturing-Special Issue on Advanced Process Control, December 2007

[14] M. Sendelbach, A. Munoz, K. Bandy, D. Prager, M. Funk, Integrated Scatterometry in High Volume Manufacturing for Polysilicon Gate Etch Control, Proc. of SPIE Microlithography Vol 6152, 2006

[15] M. Asano, T. Koike, T. Mikami, H. Abe, T. Ikeda, Satoshi Tanaka and Shoji Mimotogi, Sampling Plan Optimization for CD Control in low k1 Lithography, Proc. of SPIE Microlithography Vol 5752, 2005

[16] M. Asano, T. Ikeda, Sampling Plan Optimization for Critical Dimension Metrology, Journal of Microlith., Microfab., Microsyst., Jul-Sep. 2006, Vol. 5 (3)

[17] Ibid from reference 9

[18] M. Asano, T. Ikeda, T. Koike, H. Abe, Evaluation of Producer's and Consumer's Risks in Scatterometry and Scanning electron Microscopy Metrology for inline Critical Dimension, Journal of Microlith., Microfab., Microsyst., Oct.-Dec.. 2006, Vol. 5 (4)
[19] R. Elliott, R. K. Nurani, Sung Jin Lee, L. Ortiz, M. Preil, J. G. Shanthikumar, T. Riley, Greg Goodwin, Sampling Plan Optimization for Detection of Lithography and Etch Process Excursions, Proc. of SPIE Microlithography Vol 3998, 2000
[20] M. Asano, T. Ikeda, T. Koike, H. Abe, "Inline CD Metrology with Combined Use of Scatterometry and CD-SEM", Proc. of SPIE Microlithography Vol 6152, 2006
[21] B. Bunday, D. Michelson, J. Allgair, A. Tam, D. Chase-Colin, A. Dajczman, O. Adan, M. Har-Zvi, CD SEM Metrology Macro CD Technology—Beyond the Average, Proceedings of SPIE 2005, v5752, pp 111-126
[22] B. Bunday, O. Adan, Achieving statistical validity in CD-SEM imaging, Solid State Technology, Jan 2006.
[23] H. Cramer, T. Kiers, P. Vanoppen, J. Meessen, F. Blok, M. Dusa, Total Test Repeatability: a new figure of merit for CD Metrology tools, Proc. SPIE Int. Soc. Opt. Eng. 5375, 1254, 2004
[24] G. Han, A. Brendler, S. Manfield, G. Meiring, Statistical optimization of sampling plan and its relation to OPC model accuracy, Proc. Of SPIE, Vol. 518, pp. 651871/1-651878/10, 2007
[25] G. Vasik, O. Menedeva, D. , O. Lindman, W. Nemadi, G. Bailey, G. Studavar, SEM/contour based OPC model calibration through the process window, Proc. Of SPIE, vol. 6518, pp65187D/1-10
[26] M. Sendelbach, C. Archie, Scatterometry Measurement Precision and Accuracy Below 70 nm, *SPIE: Metrology, Inspection, and Process Control for Microlithography XVII*, ***v5035***, pp 224–238, 2003
[27] B. Bunday, B. Singh, C. Archie, W. Banke, C. Hartig, G. Cao, J. Villarrubia, M. Postek, A. Vladar, Unified Advanced CD–SEM Specification for Sub-65 nm Technology (2007 Version). ISMI document #04114595D-ENG, Dec 2007.
[28] B. Bunday, J. Allgair, B. Banke, C. Archie, R. Silver, Unified Advanced Optical Critical Dimension (OCD) Scatterometry Specification for Sub-65nm Node Technology (2007 version), ISMI document #04114596D-ENG, Dec 2007.
[29] B. Bunday, A. Peterson, J. Allgair, Specifications, Methodologies and Results of Evaluation of Optical Critical Dimension Scatterometer Tools at the 90nm CMOS Technology Node and Beyond, SPIE, ***v5752***, pp 304-323, 2005
[30] N. Orji, R. Dixson, A. Martinez, B. Bunday, J. Allgair, T. Vorburger, Progress on implementation of a reference measurement system based on a critical-dimension atomic force microscope, J. Micro/Nanolith. MEMS MOEMS 6_2_, 023002, Apr–Jun 2007
[31] B. Bunday, O. Sorkhabi, Y. Wen, A. Paranjpe, P. Terbeek, J. Allgair, A. Peterson, Improvement in Total Measurement Uncertainty for Gate CD Control, Procedings of SPIE 2005, v5878, pp 0M-1 to 0M-12
[32] SEMI E89-0999 Standard: Guide for Measurement System Capability Analysis (MSCA)

Advanced Materials Research Center, AMRC, International SEMATECH Manufacturing Initiative, and ISMI are servicemarks of SEMATECH, Inc. SEMATECH, and the SEMATECH logo are registered servicemarks of SEMATECH, Inc. All other servicemarks and trademarks are the property of their respective owners.